Simultaneous determination of Ψ and Φ angles in proteins from measurements of cross-correlated relaxation effects

Philippe Pelupessy[a], Elisabetta Chiarparin[a], Ranajeet Ghose[a] & Geoffrey Bodenhausen[a,b,*]

[a]*Section de Chimie, Université de Lausanne, BCH, CH-1015 Lausanne, Switzerland;* [b]*Département de Chimie, associé au CNRS, Ecole Normale Supérieure, 24 rue Lhomond, F-75231 Paris cedex 05, France*

Abstract

A method is presented to determine both ϕ and ψ backbone angles in proteins simultaneously. This is achieved by measuring the effect on two-spin coherences of cross-correlation between ^{15}N-$^1H^N$ and $^{13}C^\alpha$-$^1H^\alpha$ vectors. The cross-correlation rates are obtained by comparing two complementary three-dimensional experiments.
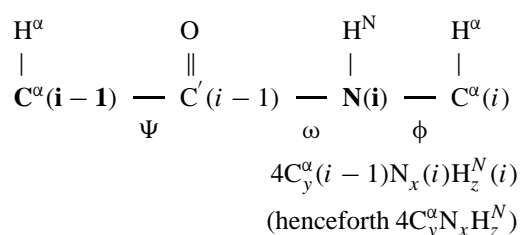
Introduction

Cross-correlation effects on two-spin coherences can be an effective probe of protein conformation (Reif et al., 1997; Yang et al., 1998; Yang and Kay, 1998; Pelupessy et al., 1999; Chiarparin et al., 1999). The extent of cross-correlation between the fluctuations of the ^{15}N-$^1H^N$ and $^{13}C^\alpha$-$^1H^\alpha$ internuclear vectors on the relaxation of zero- and double-quantum coherences involving the $^{13}C^\alpha$ nucleus of the $(i-1)$th residue of the protein and the ^{15}N nucleus of the (i)th residue depends on the backbone ψ angle (Reif et al. 1997; Yang and Kay, 1998; Pelupessy et al., 1999). Likewise, cross-correlated relaxation between the $^{13}C'$ (carbonyl) chemical shift anisotropy (CSA) and the $^{13}C^\alpha$-$^1H^\alpha$ dipolar interaction affects zero- and double-quantum coherences involving the $^{13}C^\alpha$ and $^{13}C'$ nuclei of the same amino acid also provides information on the ψ angle (Yang et al., 1998; Yang and Kay, 1998).

On the other hand, the angle ϕ is usually estimated from the magnitude of the scalar coupling $^3J(H^NH^\alpha)$, which can be measured, for example, by HNCA-J (Montelione and Wagner, 1990) or HNHA experiments (Vuister and Bax, 1993). The ϕ-angle can be correlated in an empirical fashion with $^3J(H^NH^\alpha)$ (Karplus, 1959).

In this communication, cross-correlation effects are utilized to determine *simultaneously* the backbone ϕ and ψ angles. The proposed method requires no calibration to estimate the ϕ angles, but only requires knowledge of the molecular correlation time and order paramters, which are readily available for nearly spherical proteins.

The method proposed here relies on the simultaneous creation of two types of two-spin coherences involving C^α and N nuclei of the protein backbone. At the start of a relaxation period T, the coherences of interest may be represented by the following schemes:

$$
\begin{array}{cccc}
H^\alpha & O & H^N & H^\alpha \\
| & \| & | & | \\
\mathbf{C^\alpha(i-1)} \!-\! & C'(i-1) \!-\! & \mathbf{N(i)} \!-\! & C^\alpha(i) \\
\Psi & \omega & \phi &
\end{array}
$$

$$4C_y^\alpha(i-1)N_x(i)H_z^N(i)$$

(henceforth $4C_y^\alpha N_x H_z^N$)

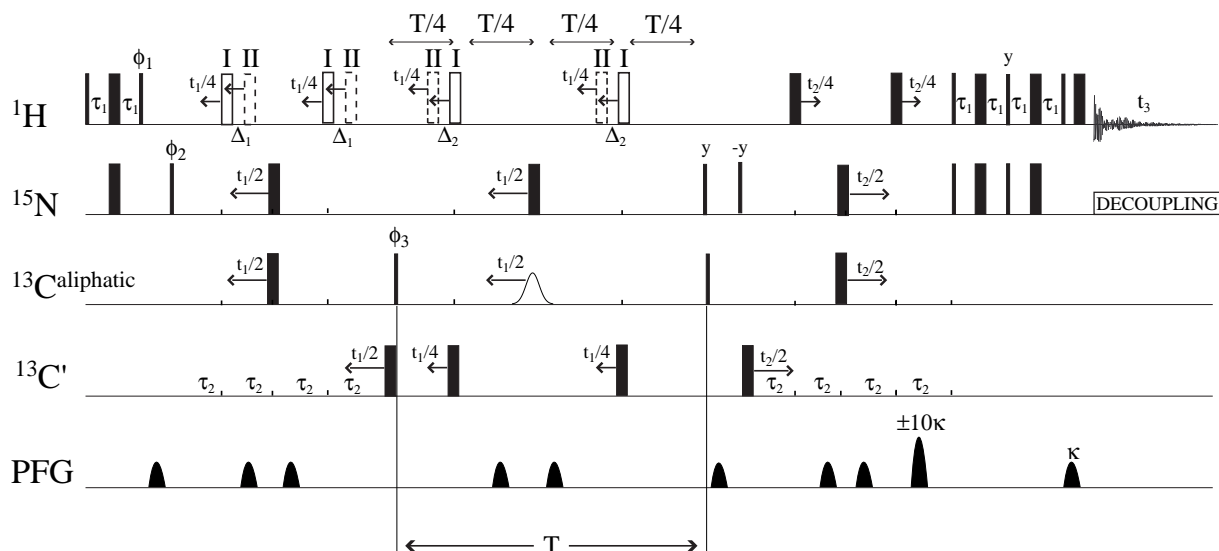*To whom correspondence should be addressed. E-mail: Geoffrey.Bodenhausen@ens.fr
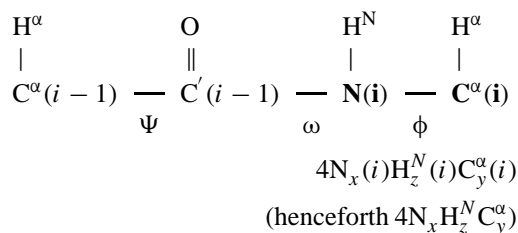
Figure 1. Pulse sequences employed for the simultaneous measurement of cross-correlation rates $R\{\theta(\phi)\}$ and $R\{\theta(\psi)\}$. Narrow and wide rectangles indicate $\pi/2$ and π pulses. The fixed delays are set to $\tau_1 = 2.5$ ms, $\tau_2 = 7.5$ ms, $\Delta_1 = 1/8J(NH^N) - 1/8J(C^\alpha H^\alpha) = 0.48$ ms and $\Delta_2 = 1/8J(C^\alpha H^\alpha) = 0.89$ ms. The bold-outlined rectangles in the experiment I are placed so that the scalar couplings are refocused. In experiment II these pulses (dashed rectangles) are shifted to allow evolution under $J(C^\alpha H^\alpha)$ and $J(NH^N)$. The $^{13}C^\alpha$ π refocusing pulse has a RE-BURP profile (Geen et al., 1991). The long and short arrows pointing to the left or right indicate that the pulses have to be shifted by $t_1/2$ and by $t_1/4$ or by $t_2/2$ and $t_2/4$. The sequences are designed to allow constant time evolution in t_1 under the ^{13}C chemical shifts. The evolution in the ^{15}N dimension occurs in t_2 in a constant time manner during the conversion of $C_z^\alpha N_x H_z^N$ and $N_x H_z^N C_z^\alpha$ into $N_y H_z^N$. Unless specified otherwise, all pulses are applied along the x-axis. The phase cycle is: $\Phi_1 = y, -y, y, -y, y, -y, y, -y$; $\Phi_2 = x, x, -x, -x, x, x, -x, -x$; $\Phi_3 = x, x, x, x, -x, -x, -x, -x$, with concomitant alternation of the receiver phase.

$$
\begin{array}{cccc}
H^\alpha & O & H^N & H^\alpha \\
| & \| & | & | \\
C^\alpha(i-1) - & C'(i-1) - & N(i) - & C^\alpha(i) \\
\Psi & \omega & & \phi
\end{array}
$$

$$4N_x(i)H_z^N(i)C_y^\alpha(i)$$

(henceforth $4N_x H_z^N C_y^\alpha$)

By ordering the operators in the sequence in which the atoms appear in the backbone it is possible to drop the indices $(i-1)$ and (i). Dipole-dipole cross-correlation between the $C^\alpha H^\alpha$ and NH^N vectors during the delay T partly converts $4C_y^\alpha N_x H_z^N$ into $4C_x^\alpha H_z^\alpha N_y$ and $4N_x H_z^N C_y^\alpha$ into $4N_y C_x^\alpha H_z^\alpha$. Assuming isotropic overall tumbling, the rate of this conversion depends on the angle θ between the $C^\alpha H^\alpha$ and NH^N vectors:

$$R(\theta) = \left(\frac{\mu_0 \hbar}{4\pi}\right)^2 \frac{\gamma_H^2 \gamma_C \gamma_N}{r_{NH}^3 r_{CH}^3} \frac{(3\cos^2\theta - 1)}{2} \frac{2S^2 \tau_c}{5}, \quad (1)$$

where S^2 is the generalized order parameter and where τ_c is the global correlation time. All other symbols

have their usual meaning. For non-spherical proteins with anisotropic tumbling the dependence of the relaxation rates on the angles θ is less straightforward (Daragan and Mayo, 1997; Ghose et al., 1998). Equation (1) applies to both $4C_y^\alpha N_x H_z^N$ and $4N_x H_z^N C_y^\alpha$ coherences. If the C^α belongs to the previous residue, θ is related to the ψ:

$$\cos(\theta) = 0.163 + 0.819 \cos(\Psi - 120°), \quad (2)$$

where it has been assumed that $\omega = 180°$, i.e. that the peptide bond is planar. On the other hand, if the C^α and N nuclei belong to the same residue, θ depends on the ϕ angle:

$$\cos(\theta) = -0.163 + 0.819 \cos(\phi - 60°). \quad (3)$$

A set of two complementary three-dimensional experiments has been designed to excite simultaneously the terms $4C_y^\alpha N_x H_z^N$ and $4N_x H_z^N C_y^\alpha$ and to measure the conversion processes $4C_y^\alpha N_x H_z^N \rightarrow 4C_x^\alpha H_z^\alpha N_y$ and $4N_x H_z^N C_y^\alpha \rightarrow 4N_y C_x^\alpha H_z^\alpha$. The pulse sequences are shown in Figure 1. The magnetization of the amide $^1H^N$ is transferred to ^{15}N and then *simultaneously*

to the $^{13}C^\alpha$'s of the same (i)th and of the previous ($i-1$)th residue in the fashion of an HNCA experiment (Kay et al., 1990), through $^1J(NC^\alpha) \sim 7\text{--}11$ Hz and $^2J(C^\alpha N) \sim 4\text{--}9$ Hz. At this stage of the sequence, there are four relevant components: $2N_yH_z^N$, $4C_z^\alpha N_xH_z^N$, $4N_xH_z^NC_z^\alpha$ and $8C_z^\alpha N_yH_z^NC_z^\alpha$. A transfer delay of 30 ms is chosen in order to maximize the amplitude of the second and third terms, while the offspring of the first and fourth terms is later eliminated by phase-cycling. Two-spin coherences $4C_y^\alpha N_xH_z^N$ and $4N_xH_z^NC_y^\alpha$ are then excited by the application of a ^{13}C $(\pi/2)_x$ pulse. Experiment I is designed to measure signals proportional to the initial terms $S_I = \langle 4C_y^\alpha N_xH_z^N \rangle$ and $S_I = \langle 4N_xH_z^NC_y^\alpha \rangle$ while experiment II allows one to measure signals arising from cross-correlation $S_{II} = \langle 4C_x^\alpha N_yH_z^\alpha \rangle$ and $S_{II} = \langle 4N_yC_x^\alpha H_z^\alpha \rangle$ in analogy to similar experiments (Felli et al., 1999; Pelupessy et al., 1999; Chiarparin et al., 1999). The difference between the two experiments lies only in the position of the proton π pulses (see Figure 1). The experiments have the same overall length and show identical relaxation behavior during the delays, but differ only in the evolution under scalar couplings. In experiment I all scalar couplings are refocused, while in experiment II, $J(C^\alpha H^\alpha)$ is active during $4\Delta_2 = 1/2J(C^\alpha H^\alpha)$ and $J(NH^N)$ during $4(\Delta_2 + \Delta_1) = 1/2J(NH^N)$. The ratio of the signal intensities of the two experiments is related to the cross-correlation rates:

$$S_{II}(4C_x^\alpha H_z^\alpha N_y)/S_I(4C_y^\alpha N_xH_z^\alpha) =$$
$$- \tanh\{R[\theta(\phi)]T\} = -[\exp\{R[\theta(\phi)]T\}$$
$$- \exp\{-R[\theta(\phi)]T\}]/[\exp\{R[\theta(\phi)]T\}$$
$$+ \exp\{-R[\theta(\phi)]T\}], \qquad (4)$$

$$S_{II}(4N_yC_x^\alpha H_z^\alpha)/S_I(4N_xH_z^NC_y^\alpha) =$$
$$- \tanh\{R[\theta(\Psi)]T\} = -[\exp\{R[\theta(\Psi)]T\}$$
$$- \exp\{-R[\theta(\Psi)]T\}]/[\exp\{R[\theta(\Psi)]T\}$$
$$+ \exp\{-R[\theta(\Psi)]T\}]. \qquad (5)$$

Evolution of the $^{13}C^\alpha$ chemical shift in t_1 allows separation of terms in Equation (4) which arise from $C^\alpha(i)$ from those in Equation (5) which arise from $C^\alpha(i-1)$. The band-selective carbon π pulse (Geen et al., 1991) in the relaxation period T inverts only the C^α region, so that the duration of the relaxation period T need not be a multiple of $1/J(C^\alpha C^\beta)$ (Yang et al., 1998). Note that $J(C^\alpha C^\beta)$ evolution occurs in t_1, since the band-selective π pulse is shifted by $t_1/2$. It

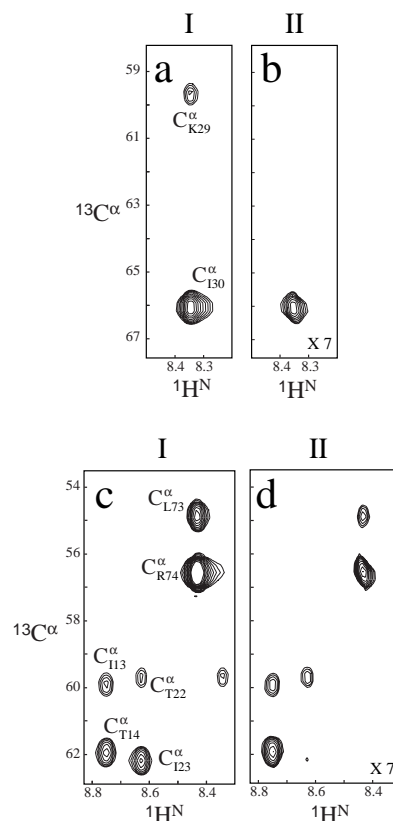*Figure 2.* Representative planes through three-dimensional spectra at selected ^{15}N chemical shifts, showing $^{13}C^\alpha$ resonances that belong to a few selected amino-acid residues and to the previous residue for Experiment I (a, c) and II (b, d). (a) and (b) correspond to a ^{15}N chemical shift of 121.2 ppm in ω_2, (c) and (d) correspond to $\omega_2 = 121.4$ ppm. The selected residues are Isoleucine-30 and Lysine-29 (I30 and K29, in the middle of an α helix), Threonine-14 and Isoleucine-13 (T14 and I13, in a β sheet), Isoleucine-23 and Threonine-22 (I23 and T22, at the start of an α helix), Arginine-74 and Leucine-73 (R74 and L73, in a loop). (c) and (d) show signals of six residues, because the ^{15}N shifts of T14, I23 and R74 are nearly degenerate around 121.4 ppm.

is possible to prevent this evolution by inserting some additional pulses, but this was not deemed useful since $J(C^\alpha C^\beta) \sim 35$ Hz is much smaller than the digital resolution in our experiments (~ 95 Hz). The position of the ^1H pulses in both experiments I and II is such that the effects of CSA/DD cross-correlations are averaged out. A z-filter is inserted to purge unwanted components. Evolution of the ^{15}N chemical shift in a constant-time fashion in t_2 during the conversion processes $4C_z^\alpha N_xH_z^N \to 2N_yH_z^N$ and $4N_xH_z^NC_z^\alpha \to 2N_yH_z^N$ allows further dispersion of resonances. Thus, in both experiments, we obtain spectra in which each amide H^N proton observed in ω_3 is correlated with
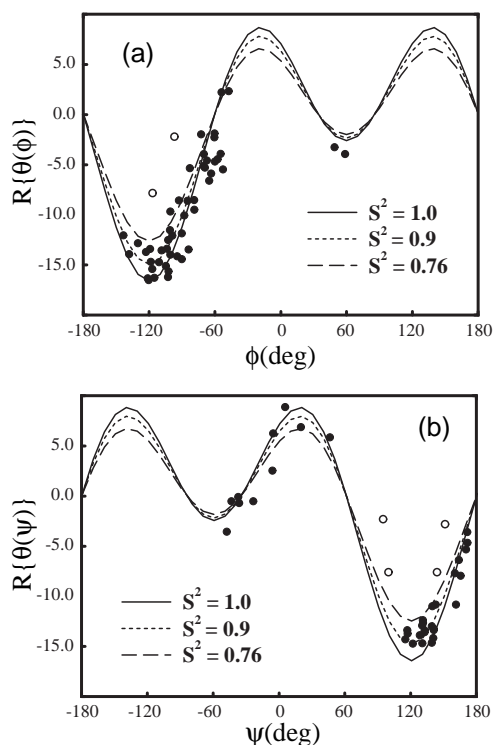
Figure 3. Experimental cross-correlation rates in ubiquitin at 303 K and 9.3 T (a) $R\{\theta(\phi)\}$ plotted as a function of the backbone angle ϕ and (b) $R\{\theta(\psi)\}$ plotted as a function of the backbone angle ψ, obtained with the sequence of Figure 1 with a Bruker Avance 400 MHz spectrometer. The rates corresponding to the four residues in the C-terminal loop which have small order parameters are indicated by open circles. In both indirect dimensions, 48 complex points were acquired. The relaxation period T was 15 ms. The angles for the appropriate amino acids were taken from the X-ray structure of ubiquitin. The curves represent the theoretical dependence predicted from Equations (1)–(3). The overall correlation time τ_c was assumed to be 4 ns. The three curves correspond to order parameters $S^2 = 1$, 0.90 and 0.76.

its ^{15}N in ω_2 and with the $^{13}C^{\alpha}$ of its own and of the $^{13}C^{\alpha}$ of the previous amino-acid residue in ω_1. Cross-peaks of a few residues belonging to different secondary structural elements of the protein are shown in Figure 2. For a given residue, the cross-peak corresponding to its own $^{13}C^{\alpha}$ is more intense than that corresponding to the $^{13}C^{\alpha}$ of the previous residue, thus making this method more accurate for determining ϕ-angles.

Figure 3 shows the cross-correlation rates measured in ^{13}C,^{15}N-labeled human ubiquitin as a function of the angles ϕ (Figure 3a) and ψ (Figure 3b), both of which were taken from the X-ray structure for the relevant amino acids (Vijay-Kumar et al., 1987). The average error for the two measured rates is

0.34 s^{-1} for $R\{\theta(\phi)\}$ and 0.83 s^{-1} for $R\{\theta(\psi)\}$. Also shown are the rates $R\{\theta(\phi)\}$ and $R\{\theta(\psi)\}$ calculated using Equations (1)–(3). Using this method alone, it is not possible to determine the ϕ and ψ angles unambiguously, since there are several values of ϕ and ψ that are compatible with a pair of experimentally determined cross-correlation rates. This is reminiscent of the ambiguity in using so-called Karplus curves. It is possible to resolve some of this ambiguity by measuring other rates which are related to the backbone angles, as shown by Yang and Kay (1998).

In conclusion, we have proposed methods which allow the simultaneous determination of the backbone ϕ and ψ angles without having to rely on Karplus curves, by measuring dipole-dipole cross-correlation rates between $C^{\alpha}H^{\alpha}$ and NH^{N} interactions. These rates are obtained by comparing signal intensities of two complementary experiments, provided the correlation time and the order parameters can be obtained from conventional relaxation measurements.

Acknowledgements

References

Chiarparin, E., Pelupessy, P., Ghose, R. and Bodenhausen, G. (1999) *J. Am. Chem. Soc.*, in press.

Daragan, V.A. and Mayo, K.H. (1997) *Prog. NMR Spectrosc.*, **31**, 63–105.

Felli, I.C., Richter, C., Griesinger, C. and Schwalbe, H. (1999) *J. Am. Chem. Soc.*, **121**, 1956–1957.

Geen, H. and Freeman, R. (1991) *J. Magn. Reson.*, **93**, 93–141.

Ghose, R., Huang, K. and Prestegard, J.H. (1998) *J. Magn. Reson.*, **135**, 487–499.

Karplus, M.J. (1959) *J. Phys. Chem.*, **30**, 11–15.

Kay, L.E., Ikura, M., Tschudin, R. and Bax, A. (1990) *J. Magn. Reson.*, **89**, 496–514.

Montelione, G. and Wagner, G. (1989) *J. Am. Chem. Soc.*, **111**, 5474–5475.

Pelupessy, P., Chiarparin, E., Ghose, R. and Bodenhausen, G. (1999) *J. Biomol. NMR*, **13**, 375–380.

Reif, B., Hennig, M. and Griesinger, C. (1997) *Science*, **276**, 1230–1233.

Vijay-Kumar, S., Bugg, C.E. and Cook, C.J. (1987) *J. Mol. Biol.*, **194**, 531–534.

Vuister, G. and Bax, A. (1993) *J. Am. Chem. Soc.*, **115**, 7772–7777.

Yang, D., Gardner, K. and Kay, L.E. (1998) *J. Biomol. NMR*, **11**, 213–220.

Yang, D. and Kay, L.E. (1998) *J. Am. Chem. Soc.*, **120**, 9880–9887.